

Massive Dirac particles based on gapped graphene with Rosen-Morse potential in a uniform magnetic field

A. Kalani, Alireza Amani, and M. A. Ramzanpour

Citation: Chin. Phys. B, 2024, 33 (**8**): 080303. DOI: 10.1088/1674-1056/ad426b
Journal homepage: http://cpb.iphy.ac.cn; http://iopscience.iop.org/cpb

What follows is a list of articles you may be interested in

Chiral bound states in a staggered array of coupled resonators

Wu-Lin Jin(金伍林), Jing Li(李静), Jing Lu(卢竞), Zhi-Rui Gong(龚志瑞), and Lan Zhou(周兰)
Chin. Phys. B, 2024, 33 (**2**): 020302. DOI: 10.1088/1674-1056/ad0bf0

Wave function collapses and 1/*n* energy spectrum induced by a Coulomb potential in a one-dimensional flat band system

Yi-Cai Zhang(张义财)
Chin. Phys. B, 2022, 31 (**5**): 050311. DOI: 10.1088/1674-1056/ac3653

Pseudospin symmetric solutions of the Dirac equation with the modified Rosen—Morse potential using Nikiforov—Uvarov method and supersymmetric quantum mechanics approach

Wen-Li Chen(陈文利) and I B Okon
Chin. Phys. B, 2022, 31 (**5**): 050302. DOI: 10.1088/1674-1056/ac2f33

Creation and annihilation phenomena of electron and positron pairs in an oscillating field

M Jiang(江淼), D D Su(苏丹丹), N S Lin(林南省), and Y J Li(李英骏)
Chin. Phys. B, 2021, 30 (**7**): 070306. DOI: 10.1088/1674-1056/abe378

Statistical properties of coherent photon-subtracted two-mode squeezed vacuum and its application in quantum teleportation

Zhang Guo-Ping (张国平), Zheng Kai-Min (郑凯敏), Liu Shi-You (刘世右), Hu Li-Yun (胡利云)
Chin. Phys. B, 2014, 23 (**5**): 050301. DOI: 10.1088/1674-1056/23/5/050301

Massive Dirac particles based on gapped graphene with Rosen–Morse potential in a uniform magnetic field

A. Kalani, Alireza Amani[†], and M. A. Ramzanpour

Department of Physics, Ayatollah Amoli Branch, Islamic Azad University, Amol, Iran

(Received 3 January 2024; revised manuscript received 6 April 2024; accepted manuscript online 24 April 2024)

We explore the gapped graphene structure in the two-dimensional plane in the presence of the Rosen–Morse potential and an external uniform magnetic field. In order to describe the corresponding structure, we consider the propagation of electrons in graphene as relativistic fermion quasi-particles, and analyze it by the wave functions of two-component spinors with pseudo-spin symmetry using the Dirac equation. Next, to solve and analyze the Dirac equation, we obtain the eigenvalues and eigenvectors using the Legendre differential equation. After that, we obtain the bounded states of energy depending on the coefficients of Rosen–Morse and magnetic potentials in terms of quantum numbers of principal n and spin–orbit k. Then, the values of the energy spectrum for the ground state and the first excited state are calculated, and the wave functions and the corresponding probabilities are plotted in terms of coordinates r. In what follows, we explore the band structure of gapped graphene by the modified dispersion relation and write it in terms of the two-dimensional wave vectors K_x and K_y. Finally, the energy bands are plotted in terms of the wave vectors K_x and K_y with and without the magnetic term.

Keywords: massive Dirac equation, Rosen–Morse potential, Legendre polynomial, gapped graphene, pseudo-spin symmetry

PACS: 03.65.Pm, 02.30.Gp, 72.80.Vp, 31.30.J– **DOI:** 10.1088/1674-1056/ad426b

1. Introduction

Today, graphene is a widely used material due to its excellent electronic, optical, thermal and mechanical properties. The structure of this substance is one of the allotropes of carbon, which is formed in a two-dimensional plane of carbon in the form of a honeycomb network. Each carbon atom has three covalent bonds with three other carbon atoms and shares one free electron between all atoms. In this case, free electrons in graphene exhibit relativistic behavior and follow the Dirac equation. Therefore, for the analysis of relativistic fermions in graphene, the Dirac equation is implemented with two approaches as massless graphene and massive graphene. The mass terms in massless and massive graphenes are zero and nonzero, respectively, which means that the variation of energy has a linear and quadratic relationship in terms of momentum, respectively. In this case, the corresponding Dirac fermions have the normal and anomalous electronic properties, respectively. The noteworthy point is that in massive graphene, the Dirac fermion has a variable speed that can approach the speed of light, but this speed is reduced to one hundredth in massless graphene compared to massive state.[1–3]

In order to describe the movement of graphene fermions, we need to obtain the relativistic wave equation with the Dirac equation. The solution of Dirac's equation has certain complexities that some potentials have analytical solutions and with some other potentials the solutions are not analytical, so we can sometimes reach analytical solutions with mathematical tricks and initiatives. Many studies solved the Dirac equation analytically and quasi-analytically, such as the Hulthén potential,[4,5] the Woods–Saxon potential,[6] the Eckart potential,[7] the Pöschl–Teller potential,[8] the Manning–Rosen potential,[9] the hyperbolic potential,[10] the Rosen–Morse potential,[11–13] the pseudo-harmonic potential,[14] and the Morse potential.[15–18] These solutions were not necessarily for graphene but for a system with fermions moving under these potentials. It should be noted that the aforesaid potentials are even solved in some physical systems by the supersymmetry method, iteration method, and Nikiforov–Uvarov method, etc.[17–20] If we pay attention to the root of the Dirac equation, it includes two potentials of repulsion vector $V(r)$ and attraction scalar $S(r)$, which are useful for determining spin and pseudo-spin symmetry, so that the vector potential and the scalar potential are coupled to mass and energy, respectively. These expressions exist in the Dirac Hamiltonian, which is invariant under the SU(2) algebra for the above-mentioned two symmetries. The corresponding symmetries with the nuclear shell model for nuclear physics phenomena were introduced by Refs. [21,22]. This means that in spin symmetry, the difference between vector and scalar potentials is constant, while in pseudo-spin symmetry the sum of these two potentials is constant.[23–25] In addition, the Dirac equation with spin symmetry and pseudo-spin symmetry has been solved with different potentials and with multiple methods.[26–30]

Now, physically, we can ask how does pseudo-spin sym-

[†]Corresponding author. E-mail: al.amani@iau.ac.ir

© 2024 Chinese Physical Society and IOP Publishing Ltd

metry happen? To answer this question, we look at the motion of electrons inside a solid and assign them an effective mass as they move through undisturbed free space. So, we come to the conclusion that the effective mass contains a different mass, which is called a quasi-particle. Therefore, the movement of electrons in a solid is the movement of quasi-particles with their effective mass. This issue is very applicable to the structure of graphene, which is a honeycomb network of individual carbon atoms. Therefore, electrons move in graphene as relativistic fermionic particles of carbon atoms that are located in the neighborhood of the Fermi level and at the edges of the first Brillouin zone, these points at the edges are called Dirac points. If we pay attention to the solutions of the Dirac equation without mass, we find that the conduction and valence bands will be in touch with each other at the Dirac points, or in other words it has a zero-energy gap. If we consider the corresponding graphene in a more realistic way, meaning that its quasi-particles have effective mass and are subjected to atomic potentials, we will see that an energy gap will be created between the conduction and valence bands, which is so-called the gapped graphene.[31–33]

In order to perform a complete and accurate investigation of graphene, the effects of electron–electron interaction as quasi-particle motion are very important. For this purpose, the electronic structures of gapped graphene can be investigated from the perspective of high energy physics, which is a meaningful bridge to condensed matter[34–36] in the sense that the quasi-particles are placed in front of a potential barrier, which prompts us to consider the corresponding system as a diatomic molecule. It should be noted that many papers have studied diatomic molecular systems in the different fields of physics using Dirac equation, Schrödinger equation, and Klein–Gordon equation.[20,37,38] Therefore, with this point of view, in this paper we study the general state of the gapped graphene under a potential barrier called Rosen–Morse potential that can describe the interatomic interaction and inter-surface interaction for quasi-particles in pseudo-spin symmetry. Rosen and Morse studied the corresponding potential for the vibrations of polyatomic molecules, such as the vibration of nitrogen inside the ammonia molecule.[11] In addition, we consider the present study in a uniform magnetic field, which causes changes in the band gap and the energy spectrum.[39–41] Since the Rosen–Morse potential is a potential that depends on the distance, it can be a very useful description of the intra-material interactions in the realistic graphene arrangement. Although the theoretical modeling was discussed in this research, it is expected that in a realistic graphene it will bring features regarding the interaction of electrons and network structure or between electrons and external fields, both electric and magnetic. Therefore, the potential can be designed to investigate the anharmonic nature and characteristics of these interactions. However, to make a graphene with Rosen–Morse potential, computational methods such as molecular dynamics simulation or quantum mechanical calculations are usually used to adapt the potential parameters to the specific properties and behaviors observed in graphene. Thus, it is possible to obtain the depth and width of the potential well by matching the range of the graphene network. However, theoretical models can provide a more accurate insight into the properties and behavior of a realistic graphene. Therefore, in this paper we solve analytically the corresponding Dirac equation in the presence of the Rosen–Morse potential and the external magnetic field for a gapped graphene. In addition, the wave functions are obtained by the Legendre polynomial as a special function and then the bound energy in terms of the coefficients related to the corresponding potential and the magnetic field.

We organize the present study as follows. In Section 2, we generally present the massive Dirac equation in the presence of the scalar and vector potentials and the magnetic field. In Section 3, we will obtain the energy spectrum and wave functions by using the Legendre polynomial in an interatomic-surface interaction by the Rosen–Morse potential as pseudo-spin symmetry, as a result we calculate the energy spectrum in terms of orbit–spin quantum numbers and draw the wave functions in terms of radial coordinates. In Section 4, we present the band structure of gapped graphene and draw the energy bands in terms of wave vectors. Finally, we provide a summary of the present work in Section 5.

2. Massive Dirac equation with an external magnetic field

In this section, we intend to consider the motion of an electron with mass M with the Fermi velocity, $v_{\rm F} \simeq 10^6$ m/s, under a scalar potential, $S(r)$, and a vector potential, $V(r)$, in an external uniform magnetic field, $\boldsymbol{B} = B_0\hat{z}$, with magnetic vector potential, $\boldsymbol{A}$, in graphene. In that case, we can write the Dirac equation with the linear momentum operator, $\boldsymbol{p}$, in the following Hamiltonian form:

$$H = v_{\rm F}\,\boldsymbol{\alpha}\cdot\left(\boldsymbol{p}-\frac{e}{c}\boldsymbol{A}\right)+\beta\left(Mc^2+S(r)\right)+V(r), \tag{1}$$

where

$$\alpha = \begin{pmatrix} 0 & \sigma \\ \sigma & 0 \end{pmatrix}, \quad \beta = \begin{pmatrix} I & 0 \\ 0 & -I \end{pmatrix} \tag{2}$$

are 4×4 matrices in which σ and I are, respectively, Pauli matrices and unitary matrix, as below:

$$\sigma_x = \begin{pmatrix} 0 & 1 \\ 1 & 0 \end{pmatrix}, \quad \sigma_y = \begin{pmatrix} 0 & -\mathrm{i} \\ \mathrm{i} & 0 \end{pmatrix},$$
$$\sigma_z = \begin{pmatrix} 1 & 0 \\ 0 & -1 \end{pmatrix}, \quad I = \begin{pmatrix} 1 & 0 \\ 0 & 1 \end{pmatrix}. \tag{3}$$

Notice that in the above Dirac equation, the radial coordinate r is on the two-dimensional plane of x–y. Now the Dirac Hamiltonian (1) is written as

$$H\Psi(r,\phi) = E\Psi(r,\phi), \tag{4}$$

where E is the eigenvalue, and $\Psi(r,\phi) = \binom{\Psi_{\rm I}(r,\phi)}{\Psi_{\rm II}(r,\phi)}$ is the wave function which one split to two-component spinors as $\Psi_{\rm I}$ and $\Psi_{\rm II}$. To insert Eqs. (1) and (2) into Eq. (4), we have

$$\Psi_{\rm I} = \frac{v_{\rm F}\,\boldsymbol{\sigma}\cdot\left(p-\frac{e}{c}A\right)}{E-Mc^2-S(r)-V(r)}\Psi_{\rm II}, \tag{5a}$$

$$\Psi_{\rm II} = \frac{v_{\rm F}\,\boldsymbol{\sigma}\cdot\left(p-\frac{e}{c}A\right)}{E+Mc^2+S(r)-V(r)}\Psi_{\rm I}, \tag{5b}$$

where the solution of the pure Dirac equation is obtained by omitting the scalar potential, the vector potential, and the magnetic vector potential in the form

$$E^{\pm} = \pm\sqrt{M^2c^4+v_{\rm F}^2p^2}, \tag{6}$$

but the solution of the above Dirac equation is laborious in the existence of the corresponding potentials; however, we obtain dispersion relation by using $\boldsymbol{\sigma}\cdot a\ \boldsymbol{\sigma}\cdot b = a\cdot b + {\rm i}\boldsymbol{\sigma}[a\times b]$ as follows:

$$\begin{aligned}&\left(E-Mc^2-S-V\right)\left(E+Mc^2+S-V\right)\\ &= v_{\rm F}^2\left(\boldsymbol{p}-\frac{e}{c}\boldsymbol{A}\right)^2.\end{aligned} \tag{7}$$

Now, in order to calculate wave function and eigenvalues of the corresponding system, we separate two-component spinor $\Psi_{\rm I}$ and $\Psi_{\rm II}$ in terms of coordinates r and ϕ in the following form:[42]

$$\begin{pmatrix}\Psi_{\rm I}(r,\phi)\\ \Psi_{\rm II}(r,\phi)\end{pmatrix} = \begin{pmatrix}\psi_1(r)\,{\rm e}^{{\rm i}k\phi}\\ {\rm i}\,\psi_2(r)\,{\rm e}^{{\rm i}(k+1)\phi}\end{pmatrix}, \tag{8}$$

where ψ_1 and ψ_2 are the radial part of the wave functions, and k is introduced spin–orbit quantum number which is a constant. Since we will consider the motion of a particle in graphene to be two-dimensional, we convert the polar coordinate r–ϕ as the Cartesian coordinates x–y as

$$\frac{\partial}{\partial x} = \cos\phi\frac{\partial}{\partial r} - \frac{\sin\phi}{r}\frac{\partial}{\partial\phi}, \tag{9a}$$

$$\frac{\partial}{\partial y} = \sin\phi\frac{\partial}{\partial r} + \frac{\cos\phi}{r}\frac{\partial}{\partial\phi}, \tag{9b}$$

and on the other we have according to coordinates x and y as

$$\boldsymbol{\sigma}\cdot\boldsymbol{p} = \sigma_x p_x + \sigma_y p_y, \tag{10}$$

where $p_x = -{\rm i}\hbar\frac{\partial}{\partial x}$ and $p_y = -{\rm i}\hbar\frac{\partial}{\partial y}$. The magnetic vector potential, $\boldsymbol{A}$, for a charged particle moving in a constant magnetic field, $\boldsymbol{\nabla}\times\boldsymbol{A} = \boldsymbol{B} = B_0\hat{z}$, to be

$$\boldsymbol{A} = \frac{1}{2}(\boldsymbol{B}\times\boldsymbol{r}). \tag{11}$$

By substituting Eqs. (8)–(11) into (4), we obtain two coupled first-order differential equations for ψ_1 and ψ_2 in the following form:

$$(\widetilde{m}-\widetilde{E}+\widetilde{S}+\widetilde{V})\psi_1 + \left(\frac{\rm d}{{\rm d}r}+\frac{k+1}{r}-\eta r\right)\psi_2 = 0, \tag{12a}$$

$$\left(\widetilde{m}+\widetilde{E}+\widetilde{S}-\widetilde{V}\right)\psi_2 + \left(\frac{\rm d}{{\rm d}r}-\frac{k}{r}+\eta r\right)\psi_1 = 0, \tag{12b}$$

where $\widetilde{E} = \frac{E}{v_{\rm F}\hbar}$, $\widetilde{m} = \frac{Mc^2}{v_{\rm F}\hbar}$, $\widetilde{V} = \frac{V}{v_{\rm F}\hbar}$, $\widetilde{S} = \frac{S}{v_{\rm F}\hbar}$, and $\eta = \frac{eB_0}{2c\hbar}$. The wave functions ψ_1 and ψ_2 are written together as

$$\psi_1 = \frac{1}{\widetilde{E}-\widetilde{m}-U(r)}\left(\frac{\rm d}{{\rm d}r}+\frac{k+1}{r}-\eta r\right)\psi_2, \tag{13a}$$

$$\psi_2 = \frac{1}{-\widetilde{E}-\widetilde{m}+W(r)}\left(\frac{\rm d}{{\rm d}r}-\frac{k}{r}+\eta r\right)\psi_1, \tag{13b}$$

where $U(r) = \widetilde{V}(r)+\widetilde{S}(r)$ and $W(r) = \widetilde{V}(r)-\widetilde{S}(r)$. We write two second-order differential equations from Eq. (13) in the following form:

$$\begin{aligned}&\frac{{\rm d}^2\psi_1}{{\rm d}r^2} + \left(\frac{1}{\widetilde{E}+\widetilde{m}-W}\frac{{\rm d}W}{{\rm d}r}+\frac{1}{r}\right)\frac{{\rm d}\psi_1}{{\rm d}r}\\ &+\left(\eta+\frac{k}{r^2}+\left(\eta r-\frac{k}{r}\right)\right.\\ &\times\left(\frac{1}{\widetilde{E}+\widetilde{m}-W}\frac{{\rm d}W}{{\rm d}r}+\frac{k+1}{r}-\eta r\right)\\ &\left.+\left(\widetilde{E}+\widetilde{m}-W\right)\left(\widetilde{E}-\widetilde{m}-U\right)\right)\psi_1 = 0,\end{aligned} \tag{14a}$$

$$\begin{aligned}&\frac{{\rm d}^2\psi_2}{{\rm d}r^2} + \left(\frac{1}{\widetilde{E}-\widetilde{m}-U}\frac{{\rm d}U}{{\rm d}r}+\frac{1}{r}\right)\frac{{\rm d}\psi_2}{{\rm d}r}\\ &+\left(-2\eta+\left(-\eta r+\frac{k+1}{r}\right)\right.\\ &\times\left(\frac{1}{\widetilde{E}-\widetilde{m}-U}\frac{{\rm d}U}{{\rm d}r}-\frac{k+1}{r}+\eta r\right)\\ &\left.+\left(\widetilde{E}+\widetilde{m}-W\right)\left(\widetilde{E}-\widetilde{m}-U\right)\right)\psi_2 = 0.\end{aligned} \tag{14b}$$

Since we intend to describe gapped graphene in the presence of external electric and magnetic fields by the Dirac equation, we have to consider the corresponding solution as the pseudo-spin symmetry. It should be noted that the Dirac equation has solutions of spin symmetry and pseudo-spin symmetry, in which $W(r) = C_{\rm s}$ = constant is called spin symmetry and $U(r) = C_{\rm ps}$ = constant is called pseudo-spin symmetry.[42–47] Therefore, we have $k(k+1) = l(l+1)$ and $k(k-1) = \widetilde{l}(\widetilde{l}+1)$ in which l and $\widetilde{l}$ are orbital angular momentum for spin symmetry and pseudo-spin symmetry, respectively. Herein, the total angular momentum is introduced as $j = l+s$ and $\widetilde{j} = \widetilde{l}+\widetilde{s}$ for spin symmetry and pseudo-spin symmetry, respectively, in which $s = \widetilde{s} = \pm 1/2$. We will have the corresponding relationships for spin symmetry

$$\text{aligned spin}: k = -(l+1),\quad j = l+\frac{1}{2},\quad k<0, \tag{15a}$$

$$\text{unaligned spin}: k=+l, \quad j=l-\frac{1}{2}, \quad k>0, \tag{15b}$$

where $k=+1,\pm2,\pm3,\ldots$, but for pseudo-spin symmetry yields

$$\text{aligned spin}: k=-\widetilde{l}, \quad j=\widetilde{l}-\frac{1}{2}, \quad k<0, \tag{16a}$$

$$\text{unaligned spin}: k=\widetilde{l}+1, \quad j=\widetilde{l}+\frac{1}{2}, \quad k>0, \tag{16b}$$

where $k=-1,\pm2,\pm3,\ldots$.

Therefore, since the spin of electrons in graphene plays the role of pseudo-spin symmetry, in this work we consider Dirac equation for pseudo-spin symmetry. In this case, Eq. (14b) becomes

$$\begin{aligned}&\frac{\mathrm{d}^2\psi_2}{\mathrm{d}r^2}+\frac{1}{r}\frac{\mathrm{d}\psi_2}{\mathrm{d}r}\\&+\left(-\eta^2r^2+2\eta k+\left(\widetilde{E}+\widetilde{m}-W\right)\right.\\&\left.\times\left(\widetilde{E}-\widetilde{m}-C_{\mathrm{ps}}\right)-\frac{(k+1)^2}{r^2}\right)\psi_2=0.\end{aligned} \tag{17}$$

In the next section, we obtain the eigenvalues and the eigenvectors for the present system with a known potential instead of $W(r)$.

3. Energy spectrum for a Rosen–Morse potential

In this section, we intend to study the effects of external electric and magnetic fields in gapped graphene by Rosen–Morse potential. For this purpose, we have to examine the effective mass of charge carriers (the propagated electrons) as relativistic fermionic quasi-particles through the graphene hexagonal lattice. Now, in order to solve the corresponding system, we must use the Dirac equation instead of Schrödinger equation from the point of view of symmetry pseudo-spin symmetry. In that case, instead of the summation of the scalar and vector potentials, we consider the Rosen–Morse potential in the following form:[11]

$$W(r)=-V_1\,\mathrm{sech}^2(\gamma r)+V_2\tanh(\gamma r), \tag{18}$$

where V_1 and V_2 are the depth of the potential, and γ is the range of the potential. The Rosen–Morse potential has a minimum in equilibrium distance (bond length) $r_{\mathrm{e}}=-\frac{1}{\gamma}\mathrm{arctanh}\left(\frac{V_2}{2V_1}\right)$. By substituting Eq. (18) into Eq. (17), we have

$$\begin{aligned}&\frac{\mathrm{d}^2\psi_2(r)}{\mathrm{d}r^2}+\frac{1}{r}\frac{\mathrm{d}\psi_2(r)}{\mathrm{d}r}+\left(-\eta^2r^2+2\eta k-\frac{(k+1)^2}{r^2}\right.\\&+\left(\widetilde{E}+\widetilde{m}+V_1\,\mathrm{sech}^2(\gamma r)-V_2\tanh(\gamma r)\right)\\&\left.\times\left(\widetilde{E}-\widetilde{m}-C_{\mathrm{ps}}\right)\right)\psi_2(r)=0,\end{aligned} \tag{19}$$

where by changing variable $z=\tanh(\gamma r)$ and applying it to the above equation, we will have

$$\begin{aligned}&(1-z^2)\frac{\mathrm{d}^2\psi_2(z)}{\mathrm{d}z^2}-2z\frac{\mathrm{d}\psi_2(z)}{\mathrm{d}z}+\frac{1}{\mathrm{arctanh}(z)}\frac{\mathrm{d}\psi_2(z)}{\mathrm{d}z}\\&+\left(-\frac{\eta^2}{\gamma^4}\frac{\mathrm{arctanh}^2(z)}{1-z^2}+\frac{2\eta k}{\gamma^2}\frac{1}{1-z^2}\right.\\&+\left(\frac{(\widetilde{E}+\widetilde{m})}{\gamma^2}\frac{1}{1-z^2}+\frac{V_1}{\gamma^2}-\frac{V_2}{\gamma^2}\frac{z}{1-z^2}\right)\left(\widetilde{E}-\widetilde{m}-C_{\mathrm{ps}}\right)\\&\left.-\frac{(k+1)^2}{(1-z^2)\,\mathrm{arctanh}^2(z)}\right)\psi_2(z)=0.\end{aligned} \tag{20}$$

The analytical solution of the above equation is very complicated, so we can solve it by using the approximation method. Commonly in physics problems, the Taylor series is used as a powerful mathematical technique to simplify models when they are impossible to achieve. This series allows us to approximate the function near that point using a polynomial. For this purpose, we approximate trigonometric terms around $z_{\mathrm{e}}=\tanh(\gamma r_{\mathrm{e}})=-\frac{V_2}{2V_1}$ in which r_{e} is the bond length. In that case, we have

$$\begin{aligned}&\frac{1}{\mathrm{arctanh}(z)}\\&\simeq\frac{z_{\mathrm{e}}^2+z_{\mathrm{e}}(1-2z_{\mathrm{e}}^2)\,\mathrm{arctanh}(z_{\mathrm{e}})+(1-z_{\mathrm{e}}^2)^2\,\mathrm{arctanh}^2(z_{\mathrm{e}})}{(1-z_{\mathrm{e}}^2)^2\,\mathrm{arctanh}^3(z_{\mathrm{e}})}\\&-\frac{2z_{\mathrm{e}}+(1-3z_{\mathrm{e}}^2)\mathrm{arctanh}(z_{\mathrm{e}})}{(1-z_{\mathrm{e}}^2)^2\,\mathrm{arctanh}^3(z_{\mathrm{e}})}z\\&+\frac{1-z_{\mathrm{e}}\,\mathrm{arctanh}(z_{\mathrm{e}})}{(1-z_{\mathrm{e}}^2)^2\,\mathrm{arctanh}^3(z_{\mathrm{e}})}z^2+O(z)^3,\end{aligned} \tag{21a}$$

$$\begin{aligned}&\frac{\mathrm{arctanh}^2(z)}{1-z^2}\\&\simeq\frac{z_{\mathrm{e}}^2-2z_{\mathrm{e}}(1-4z_{\mathrm{e}}^2)\mathrm{arctanh}(z_{\mathrm{e}})+(1-3z_{\mathrm{e}}^2+6z_{\mathrm{e}}^4)\,\mathrm{arctanh}^2(z_{\mathrm{e}})}{(1-z_{\mathrm{e}}^2)^3}\\&+\frac{-2z_{\mathrm{e}}+2(1-7z_{\mathrm{e}}^2)\,\mathrm{arctanh}(z_{\mathrm{e}})-8z_{\mathrm{e}}^3\,\mathrm{arctanh}^2(z_{\mathrm{e}})}{(1-z_{\mathrm{e}}^2)^3}z\\&+\frac{1+6z_{\mathrm{e}}\,\mathrm{arctanh}(z_{\mathrm{e}})+(1+3z_{\mathrm{e}}^2)\,\mathrm{arctanh}^2(z_{\mathrm{e}})}{(1-z_{\mathrm{e}}^2)^3}z^2+O(z)^3,\end{aligned} \tag{21b}$$

$$\begin{aligned}&\frac{1}{(1-z^2)\,\mathrm{arctanh}^2(z)}\\&\simeq\frac{3z_{\mathrm{e}}^2+2z_{\mathrm{e}}(1-4z_{\mathrm{e}}^2)\,\mathrm{arctanh}(z_{\mathrm{e}})+(1-3z_{\mathrm{e}}^2+6z_{\mathrm{e}}^4)\,\mathrm{arctanh}^2(z_{\mathrm{e}})}{(1-z_{\mathrm{e}}^2)^3\,\mathrm{arctanh}^4(z_{\mathrm{e}})}\\&+\frac{6z_{\mathrm{e}}+2(1-7z_{\mathrm{e}}^2)\,\mathrm{arctanh}(z_{\mathrm{e}})+8z_{\mathrm{e}}^3\,\mathrm{arctanh}^2(z_{\mathrm{e}})}{(1-z_{\mathrm{e}}^2)^3\,\mathrm{arctanh}^4(z_{\mathrm{e}})}z\\&+\frac{3-6z_{\mathrm{e}}\,\mathrm{arctanh}(z_{\mathrm{e}})+(1+3z_{\mathrm{e}}^2)\,\mathrm{arctanh}^2(z_{\mathrm{e}})}{(1-z_{\mathrm{e}}^2)^3\,\mathrm{arctanh}^4(z_{\mathrm{e}})}z^2+O(z)^3.\end{aligned} \tag{21c}$$

On the other hand, we can, respectively, write the above approximation terms as

$$\frac{1}{\mathrm{arctanh}(z)}=a_0+a_1z+a_2z^2, \tag{22a}$$

$$\frac{\mathrm{arctanh}^2(z)}{1-z^2}=b_0+b_1z+b_2z^2, \tag{22b}$$

$$\frac{1}{(1-z^2)\,\mathrm{arctanh}^2(z)}=c_0+c_1z+c_2z^2. \tag{22c}$$

Now we can write down coefficients a_0 to c_2 by using Eqs. (21) and (22) in the following form:

$$a_0 = \frac{z_e^2 + z_e(1-2z_e^2)\,\mathrm{arctanh}(z_e) + (1-z_e^2)^2\,\mathrm{arctanh}^2(z_e)}{(1-z_e^2)^2\,\mathrm{arctanh}^3(z_e)}, \tag{23a}$$

$$a_1 = -\frac{2z_e + (1-3z_e^2)\mathrm{arctanh}(z_e)}{(1-z_e^2)^2\,\mathrm{arctanh}^3(z_e)}, \tag{23b}$$

$$a_2 = \frac{1 - z_e\,\mathrm{arctanh}(z_e)}{(1-z_e^2)^2\,\mathrm{arctanh}^3(z_e)}, \tag{23c}$$

$$b_0 = \frac{z_e^2 - 2z_e(1-4z_e^2)\mathrm{arctanh}(z_e) + (1-3z_e^2+6z_e^4)\,\mathrm{arctanh}^2(z_e)}{(1-z_e^2)^3}, \tag{23d}$$

$$b_1 = \frac{-2z_e + 2(1-7z_e^2)\,\mathrm{arctanh}(z_e) - 8z_e^3\,\mathrm{arctanh}^2(z_e)}{(1-z_e^2)^3}, \tag{23e}$$

$$b_2 = \frac{1 + 6z_e\,\mathrm{arctanh}(z_e) + (1+3z_e^2)\,\mathrm{arctanh}^2(z_e)}{(1-z_e^2)^3}, \tag{23f}$$

$$c_0 = \frac{3z_e^2 + 2z_e(1-4z_e^2)\,\mathrm{arctanh}(z_e) + (1-3z_e^2+6z_e^4)\,\mathrm{arctanh}^2(z_e)}{(1-z_e^2)^3\,\mathrm{arctanh}^4(z_e)}, \tag{23g}$$

$$c_1 = \frac{6z_e + 2(1-7z_e^2)\,\mathrm{arctanh}(z_e) + 8z_e^3\,\mathrm{arctanh}^2(z_e)}{(1-z_e^2)^3\,\mathrm{arctanh}^4(z_e)}, \tag{23h}$$

$$c_2 = \frac{3 - 6z_e\,\mathrm{arctanh}(z_e) + (1+3z_e^2)\,\mathrm{arctanh}^2(z_e)}{(1-z_e^2)^3\,\mathrm{arctanh}^4(z_e)}, \tag{23i}$$

where by considering the value of equilibrium distance (bond length), $r_e = 2.197224577$ fm, we can obtain coefficients a_0 to c_2 as

$$a_0 = 5.974907579, \quad a_1 = -12.19886077, \quad a_2 = 7.780005050, \tag{24a}$$

$$b_0 = 0.2579095562, \quad b_1 = -1.289505649, \quad b_2 = 2.496412480, \tag{24b}$$

$$c_0 = 23.32181071, \quad c_1 = -63.94181239, \quad c_2 = 24.53113834. \tag{24c}$$

In what follows, we will solve the corresponding system by using the separation method. For this purpose, we can write down the wave function in terms of multiplied between an arbitrary function, $R(z)$, and the Legendre polynomial, $P_n(z)$, in the form

$$\psi_2(z) = R(z)P_n(z), \tag{25}$$

where the Legendre polynomial is an orthogonal polynomial of degrees n, and its differential form is

$$(1-z^2)P_n{}''(z) - 2zP_n{}'(z) + n(n+1)P_n(z) = 0, \tag{26}$$

where one is defined over the interval $[-1, 1]$. In addition, we can write down its Rodrigues Formula as below:

$$P_n(z) = \frac{1}{2^n n!}\frac{\mathrm{d}^n}{\mathrm{d}z^n}\left((z^2-1)^n\right). \tag{27}$$

To insert Eqs. (22) and (25) into Eq. (20), one yields

$$\begin{aligned}
&(1-z^2)P_n{}''(z) \\
&+\left[2(1-z^2)\frac{R'}{R} - 2z + a_0 + a_1 z + a_2 z^2\right]P_n{}'(z) \\
&\left[(1-z^2)\frac{R''}{R} - 2z\frac{R'}{R} + (a_0 + a_1 z + a_2 z^2)\frac{R'}{R}\right. \\
&-\frac{\eta^2}{\gamma^4}(b_0 + b_1 z + b_2 z^2) + \frac{2\eta k}{\gamma^2}\frac{1}{1-z^2} \\
&+\left(\frac{(\widetilde{E}+\widetilde{m})}{\gamma^2}\frac{1}{1-z^2} + \frac{V_1}{\gamma^2} - \frac{V_2}{\gamma^2}\frac{z}{1-z^2}\right)(\widetilde{E} - \widetilde{m} - C_{\mathrm{ps}}) \\
&\left.-(k+1)^2(c_0 + c_1 z + c_2 z^2)\right]P_n(z) = 0,
\end{aligned} \tag{28}$$

where index $'$ is the derivative with respect to z.

In order to obtain the form of function $R(z)$, we consider the second term of Eq. (28) to be equivalent to the second term of Eq. (26). In that case, we have

$$R(z) = R_0\,(z-1)^{\frac{a_0+a_1+a_2}{4}}\,(z+1)^{\frac{-a_0+a_1-a_2}{4}}\,\mathrm{e}^{\frac{a_2}{2}z}, \tag{29}$$

where R_0 is introduced as an integral constant. The important feature of this solution is that the boundary condition for wave function is as $\psi(r\to 0) \neq 0$ and $\psi(r\to\infty) = 0$, i.e., the particle is present in $r\to 0$ but not in $r\to\infty$. By inserting Eq. (29) into the third term of Eq. (28), and then by equating the third term of Eq. (28) with the third term of Eq. (26), the following results are obtained:

$$\begin{aligned}
\eta^2 \;=\; &\frac{\gamma^4}{4}\left(\frac{a_2^2}{2b_1} + \frac{a_2(a_1-2)}{b_1}\right) \\
&-\frac{\gamma^4}{2}(k+1)^2\left(\frac{c_2}{b_2} + \frac{c_1}{b_1}\right),
\end{aligned} \tag{30a}$$

$$4n(n+1)+4c_0(k+1)^2-a_1^2-a_2^2+2(a_1-a_0a_2)$$
$$-\frac{4V_1}{\gamma^2}\left(\widetilde{E}-\widetilde{m}-C_{\rm ps}\right)+\frac{4b_0}{\gamma^4}\eta^2=0, \tag{30b}$$
$$\frac{4}{\gamma^2}\left(\widetilde{E}+\widetilde{m}+V_2\right)\left(\widetilde{E}-\widetilde{m}-C_{\rm ps}\right)$$
$$+\frac{8k}{\gamma^2}\eta-(a_0-a_1+a_2)^2=0, \tag{30c}$$
$$\frac{4}{\gamma^2}\left(\widetilde{E}+\widetilde{m}-V_2\right)\left(\widetilde{E}-\widetilde{m}-C_{\rm ps}\right)$$
$$+\frac{8k}{\gamma^2}\eta-(a_0+a_1+a_2)^2=0, \tag{30d}$$

where first two relations show the quantization of the magnetic field, i.e., η is written in terms of k. In addition, we obtain the energy spectra, $\widetilde{E}\equiv\widetilde{E}_{nk}$, from the combination of the last three relations in the following form:

$$\widetilde{E}_{nk} = \frac{\gamma^2}{8V_1}\left(4n(n+1)+4c_0(k+1)^2\right.$$
$$\left.+\frac{4b_0}{\gamma^4}\eta^2-(2a_0a_2+a_1^2+a_2^2-2a_1)\right)$$
$$-\frac{\gamma^2a_1}{4V_2}(a_0+a_2)+C_{\rm ps}+\widetilde{m}, \tag{31}$$

where in order to eliminate η by inserting Eq. (30a) into Eq. (31) we have

$$\widetilde{E}_{nk} = \frac{\gamma^2}{8V_1}\left[4n(n+1)+4(k+1)^2\left(2c_0-\frac{b_0c_1}{b_1}-\frac{b_0c_2}{b_2}\right)\right.$$
$$\left.+b_0\left(\frac{a_2^2}{2b_1}+\frac{a_2(a_1-2)}{b_1}\right)-(2a_0a_2+a_1^2+a_2^2-2a_1)\right]$$
$$-\frac{\gamma^2a_1}{4V_2}(a_0+a_2)+C_{\rm ps}+\widetilde{m}, \tag{32}$$

where $\widetilde{E}_{nk}$ is dependent on the Rosen–Morse and external magnetic potentials, and is written in terms of the quantum numbers and other coefficients.

Table 1. The energy spectrum $\widetilde{E}_{nk}$ by the values of $r_{\rm e}=2.197224577$ fm, $\widetilde{m}=1$ fm^{-1}, $\gamma=0.25$ fm^{-1}, $V_1=-1$ fm^{-1}, $V_2=1$ fm^{-1}, and $C_{\rm PS}=-6$ fm^{-1}.[12]

n	k	$\widetilde{l}$	$\widetilde{j}$	l	$nL_{\widetilde{j}};(n-1)L_{\widetilde{j}}$	$\widetilde{E}_{nk}$ (fm^{-1})	n	k	$\widetilde{l}$	$\widetilde{j}$	l	$nL_{\widetilde{j}};(n-1)L_{\widetilde{j}}$	$\widetilde{E}_{nk}$ (fm^{-1})
1	−4	4	7/2	3	$1f_{7/2}$	−4.489788121	2	−4	4	7/2	3	$2f_{7/2}$	−4.614788121
1	−3	3	5/2	2	$1d_{5/2}$	−2.042875755	2	−3	3	5/2	2	$2d_{5/2}$	−2.167875755
1	−2	2	3/2	1	$1p_{3/2}$	−0.574728336	2	−2	2	3/2	1	$2p_{3/2}$	−0.699728336
1	−1	1	1/2	0	$1s_{1/2}$	−0.085345864	2	−1	1	1/2	0	$2s_{1/2}$	−0.210345864
1	2	1	3/2	2	$0d_{3/2}$	−4.489788121	2	2	1	3/2	2	$1d_{3/2}$	−4.614788121
1	3	2	5/2	3	$0f_{5/2}$	−7.915465434	2	3	2	5/2	3	$1f_{5/2}$	−8.040465434
1	4	3	7/2	4	$0g_{7/2}$	−12.31990769	2	4	3	7/2	4	$1g_{7/2}$	−12.44490768
1	5	4	9/2	5	$0h_{9/2}$	−17.70311488	2	5	4	9/2	5	$1h_{9/2}$	−17.82811488

In order to have a deeper understanding of the calculations related to the energy spectrum (32), we observe its values in terms of the quantum numbers n and k as given in Table 1. As mentioned in the previous section, in this paper we are dealing with pseudo-spin symmetry merely for gapped graphene, so that with the help of Eq. (16) we can obtain a relationship between k, $\widetilde{j}$, l, and $\widetilde{l}$ in the states with aligned spin ($k<0$) and unaligned spin ($k>0$) in Table 1. We can also write down the corresponding orbitals for $L=0,1,2,3,4,5,\ldots$ with shapes s, p, d, f, g, h, …, respectively, as $nL_{\widetilde{j}}$ when $k>0$ and $(n-1)L_{\widetilde{j}}$ when $k<0$. Table 1 shows us that there is a degeneracy energy for $k\to-k-2$, so we have $\widetilde{E}_{nk}=\widetilde{E}_{n\bar{k}-2}$ in which symbol $\bar{k}$ is $-k$. In addition, we can rewrite down Eq. (32) in a more compact form as follows:

$$\widetilde{E}_{nk}=An(n+1)+B(k+1)^2+C, \tag{33}$$

where the coefficients A, B, and C are

$$A = \frac{\gamma^2}{2V_1}, \tag{34a}$$
$$B = \frac{\gamma^2}{2V_1}\left(2c_0-\frac{b_0c_1}{b_1}-\frac{b_0c_2}{b_2}\right), \tag{34b}$$
$$C = \frac{\gamma^2}{8V_1}\left(\frac{b_0a_2^2}{2b_1}+\frac{b_0a_2(a_1-2)}{b_1}-2a_0a_2-a_1^2-a_2^2+2a_1\right)$$
$$-\frac{\gamma^2a_1}{4V_2}(a_0+a_2)+C_{\rm ps}+\widetilde{m}. \tag{34c}$$

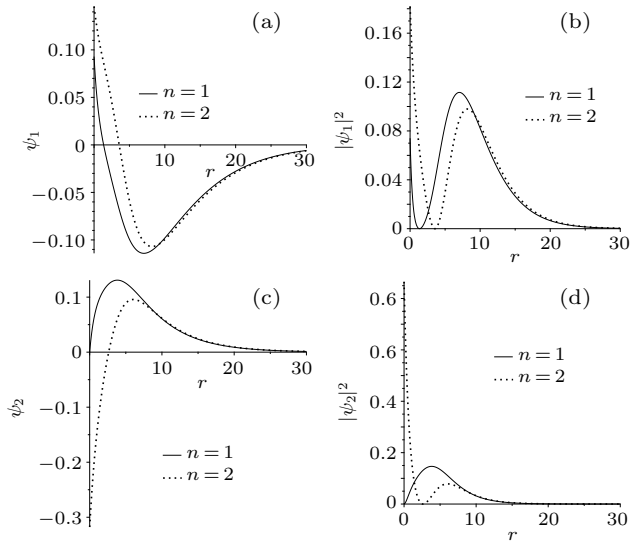


Fig. 1. The real part of the wave functions ψ_1 and ψ_2 and their probabilities in terms of coordinate r in which the ground state and the first excited state are represented by the line and the dot, respectively.

In order to represent the variation of the wave functions ψ_1 and ψ_2 in terms of coordinate r, we first obtain wave function ψ_2 by substituting Eq. (29) into Eq. (25) provided that $z = \tanh(\gamma r)$, and we then earn wave function ψ_1 by substituting the obtained ψ_2 into Eq. (13a). In that case, we can see the variation of the radial part of the wave functions ψ_1 and ψ_2, and the corresponding probabilities in terms of radial coordinate r for the principal quantum number n in Fig. 1. Figure 1 depicts us that the wave functions ψ_1 and ψ_2 tend to zero when the coordinate r tends to infinity.

4. Band structure of gapped graphene

From the perspective of relativistic quantum mechanics, the band structure of gapped graphene is an interesting topic in condensed matter physics, and even in nanotechnology. As we know, graphene composed of carbon atoms in a hexagonal honeycomb lattice is considered as a two-dimensional material that has a unique electronic property of having a zero-band gap at the Dirac points, i.e., where the valence and conduction bands are in touch with each other. Therefore, due to the aforementioned characteristics, graphene is classified as a semi-metal with high electrical properties. On the other hand, in a more realistic investigation, especially in transistors, solar cells, and sensors, we find that graphene plays the role of a semiconductor, i.e., a band gap creates between the valence and conduction bands, which is caused by factors such as defects, electric fields, and or the multi-layeredness of graphene. Therefore, the energy band gap is between the conduction and valence bands, where the conduction energy band corresponds to the energy of the electrons formed in the innermost shell of the atom, and the valence energy band corresponds to the energy of the valence electrons, which are located in the outermost part of the atomic shell.

Now, in order to explore the present work from the point of view of band structure, we note that momentum is a function of the two-dimensional wave vectors K_x and K_y, written as $\boldsymbol{p} = \hbar K_x \boldsymbol{i} + \hbar K_y \boldsymbol{j}$. In that case, by inserting the current momentum and Eq. (11) into Eq. (7), we obtain the dispersion relation for gapped graphene in the presence of the Rosen–Morse potential and magnetic field as follows:

$$\begin{aligned} &\left(\widetilde{E} - \widetilde{m} - C_{\mathrm{ps}}\right)\left(\widetilde{E} + \widetilde{m} - W\right) \\ &= K_x^2 + K_y^2 + \eta^2 r^2 + 2\eta\left(yK_x - xK_y\right), \end{aligned} \tag{35}$$

where W is the same the Rosen–Morse potential (18). Therefore, in this work, the modified dispersion relation is obtained in the presence of scalar, vector and magnetic vector potentials. However, we note that if we ignore the effects of scalar and vector potentials, and even the effective mass of electrons, graphene behaves as a massless fermion, in which case it will have a zero-energy gap. In general, a more complicated problem is to calculate the dispersion relation of gapped graphene in the presence of scalar and vector potentials than in the potential-free case, which must be calculated through wave vectors. In this case, we expect the dispersion relation to provide insight into the behavior of waves within material.

In what follows, we intend to represent band structure of gapped graphene in terms of wave vectors K_x and K_y. For this purpose, we will have that the edges of the first Brillouin zone are placed at a distance in the conduction and valence bands from each other at six points, which is so-called the gap energy of graphene, and for this reason the corresponding graphene is called gapped graphene. To show the graphene lattice vectors, we consider it as a honeycomb structure in the form of triangular lattices in a two-dimensional plane with a base of two atoms per unit cell. In this case, the network vectors, a_1 and a_2 with the lattice constant $a_0 = 1.42$ Å are as follows:[35]

$$a_1 = \frac{a_0}{2}(3, +\sqrt{3}), \tag{36a}$$

$$a_2 = \frac{a_0}{2}(3, -\sqrt{3}), \tag{36b}$$

and the reciprocal network vectors b_1 and b_2 are written in the form

$$b_1 = \frac{2\pi}{3a_0}(1, +\sqrt{3}), \tag{37a}$$

$$b_2 = \frac{2\pi}{3a_0}(1, -\sqrt{3}), \tag{37b}$$

and the coordinates of the Dirac six-point wave vectors K and K' read

$$\begin{aligned} K = &\left(+\frac{2\pi}{3a_0}, \frac{2\pi}{3\sqrt{3}a_0}\right), \left(-\frac{2\pi}{3a_0}, \frac{2\pi}{3\sqrt{3}a_0}\right), \\ &\left(0, +\frac{4\pi}{3\sqrt{3}a_0}\right), \end{aligned} \tag{38a}$$

$$\begin{aligned} K' = &\left(+\frac{2\pi}{3a_0}, -\frac{2\pi}{3\sqrt{3}a_0}\right), \left(-\frac{2\pi}{3a_0}, -\frac{2\pi}{3\sqrt{3}a_0}\right), \\ &\left(0, -\frac{4\pi}{3\sqrt{3}a_0}\right). \end{aligned} \tag{38b}$$

However, we plot the graph of the dispersion relation (35) in terms of K_x and K_y for magnetic term values of $\eta = 1$ (Fig. 2(a)) and $\eta = 0$ (Fig. 2(b)) based on the values listed in Table 1. In Fig. 2(a), we can see that there are two energy bands as the valence band and the conduction band, and the difference between the minimum value of the conduction band and the maximum value of the valence band, which is called the gap energy, is about 5.7 fm^{-1} for the component x and is about 5.4 fm^{-1} for component y. We note that the size of the band gap energy depends on the mass, potential, and magnetic term applied to it. Another point in Fig. 2 is that in both figures we see a deviation from the origin due to magnetic spins caused by magnetic fields. This means that if we omit the effect of the magnetic field into the dispersion relation (35), we will have the symmetric dispersion relation in terms of wave vectors K_x and K_y, as shown in Fig. 2(b). Therefore, in the modified dispersion relation (35), when the effect

of mass, scalar and vector potentials, and the external magnetic field are omitted in the Hamiltonian of the present work, the gapped graphene structure becomes a virgin graphene, in which case the band gap energy will be zero. We also observe that before and after the extremum points in the graph, the energy bands have a linear relationship with the wave vectors, which is one of the important features of graphene.

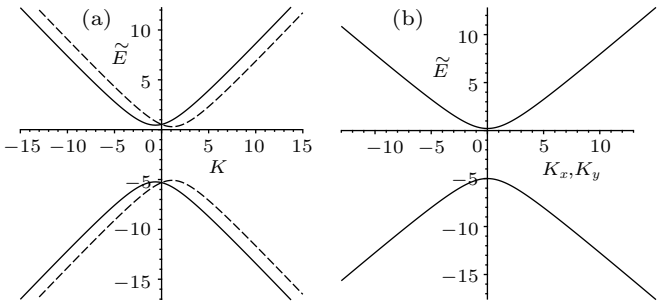


Fig. 2. (a) The energy bands in terms of wave vectors K_x (line) and K_y (dash) for $\eta = 1$. (b) The energy bands in terms of wave vectors K_x and K_y for $\eta = 0$, which are the same.

5. Conclusion

In this paper, we studied the gapped graphene structure in the context of the Dirac Hamiltonian containing terms such as mass, scalar and vector potentials, and the external uniform magnetic field. The corresponding Dirac equation has been explored in two-dimensional space and we wrote down the wave functions as the two-component spinors, so that they are expressed in terms of polar coordinate r–ϕ by an arbitrary spin–orbit quantum number k. Since the relativity Dirac equation is related to the motion of spin half particle as fermionic quasi-particles, it can describe the gapped graphene with the pseudo-spin symmetry approach as $k > 0$ for aligned spin and $k < 0$ for unaligned spin. Next, we considered the pseudo-spin symmetry as the sum of scalar and vector potentials equal to a constant value, which is written as $U(r) = C_{\rm ps}$.

Next, to solve the current system, we converted the Dirac Hamiltonian from polar coordinates r–ϕ to Cartesian coordinates x–y and then obtained two second-order differential equations in terms of the radial part of the wave functions ψ_1 and ψ_2. In order to describe the relativistic electron propagation in graphene under an interatomic potential, we considered the difference between the scalar and vector potentials as the Rosen–Morse potential (18) with bond length $r_{\rm e} = -\frac{1}{\gamma}\text{arctanh}\left(\frac{V_2}{2V_1}\right)$. Although this choice makes the present study much more difficult and complicated, it is expected to have a good achievement for the construction of graphene-based electronic devices. Afterward, we put the Rosen–Morse potential into the second-order differential equation for the wave function ψ_2, and then deformed it by changing the variable $z = \tanh(\gamma r)$ to reach an analytical solution. Then, we expand the trigonometric expressions with a good approximation by Taylor expansion around the point of bond length $z_{\rm e} = \tanh(\gamma r_{\rm e})$ up to the second order. In the next step, with the help of the separation method, we consider that the wave function is equal to the product between the arbitrary function, $R(z)$, and the Legendre polynomial, $P_n(z)$. Then, we acquired the eigenvector (29) and the eigenvalues (33) by comparing the second and the third terms of the second-order differential equations of the wave function ψ_2 and the Legendre polynomial. We note that the eigenvalues are the same as the bound states or energy spectrum, which depends on the Rosen–Morse potential and the external magnetic potential. Next, the energy spectrum has been calculated in terms of quantum numbers n and k as aligned-unaligned spins with the listed values, as shown in Table 1. We also represented the corresponding calculations for orbitals with shapes s, p, d, f, g, and h. We observe that there is a degeneracy energy for $k \to -k-2$ as $\widetilde{E}_{nk} = \widetilde{E}_{n\bar{k}-2}$, as shown in Table 1. Therefore, we plotted the graph of the wave functions ψ_1 and ψ_2, and their probabilities in terms of radial coordinate r for orbitals s and p, which are same the ground state and the first excited state, respectively.

We studied the topology of the gapped graphene band structure using the dispersion relation. For this purpose, we first obtained the modified dispersion relation from the corresponding Dirac equation in terms of the two-dimensional wave vectors K_x and K_y, and in this way we were able to describe the conduction and valence bands in this work. We note that the modified dispersion relation depends on the electron mass, the Rosen–Morse potential, and the external magnetic field. Finally, we plotted the variation of the conduction and valence bands in terms of wave vectors K_x and K_y, and then calculated the corresponding energy gap or band gap for different effects of the external magnetic field. The remarkable thing in this research was that there is a curve around the minimum and maximum points of the energy bands, but beyond that a linear relationship with the wave vector is observed.

References

[1] Khveshchenko D V 2009 *J. Phys.: Condens. Matter* **21** 075303
[2] Ulstrup S, Johannsen J C, Cilento F, Miwa J A, Crepaldi A, Zacchigna M, Cacho C, Chapman R, Springate E, Mammadov S and Fromm, F 2014 *Phys. Rev. Lett.* **112** 257401
[3] Setare M R and Jahani D 2010 *Physica B* **405** 1433
[4] Guo J Y, Meng J and Xu F X 2003 *Chin. Phys. Lett.* **20** 602
[5] Ikhdair S M and Sever R 2010 *Applied Mathematics and Computation* **216** 911
[6] Guo J Y and Sheng Z Q 2005 *Phys. Lett. A* **338** 90
[7] Sari R A, Suparmi A and Cari C 2015 *Chin. Phys. B* **25** 010301
[8] Wei G F and Dong S H 2009 *Europhys. Lett.* **87** 40004
[9] Wei G F and Dong S H 2008 *Phys. Lett. A* **373** 49
[10] Jia C S, Liu J Y, Wang P Q and Lin X 2009 *International Journal of Theoretical Physics* **48** 2633
[11] Rosen N and Morse P M 1932 *Phys. Rev.* **42** 210
[12] Ikhdair S M and Hamzavi M 2013 *Chin. Phys. B* **22** 040302
[13] Oyewumi K J and Akoshile C O 2010 *Euro. Phys. J. A* **45** 311
[14] Chen G, Chen Z D and Lou Z M 2004 *Chin. Phys.* **13** 279
[15] Morse P M 1929 *Phys. Rev.* **34** 57
[16] Zhang P, Long H C and Jia C S 2016 *Euro. Phys. J. Plus* **131** 117
[17] Berkdemir C 2006 *Nuclear Physics A* **770** 32
[18] Ikhdair S M 2011 *Journal of Mathematical Physics* **52** 122108

[19] Bayrak O and Boztosun I 2007 *J. Phys. A: Math. Theor.* **40** 11119
[20] Amani A R and Ghorbanpour H 2012 *Acta Physica Polonica-Series B Elementary Particle Physics* **43** 1795
[21] Hecht K T and Adler A 1969 *Nuclear Physics A* **137** 129
[22] Arima A, Harvey M and Shimizu K 1969 *Phys. Lett. B* **30** 517
[23] Ginocchio J N, Leviatan A, Meng J and Zhou S G 2004 *Phys. Rev. C* **69** 034303
[24] Smith G B and Tassie L J 1971 *Annals of Physics* **65** 352
[25] Bell J S and Ruegg H 1975 *Nuclear Physics B* **98** 151
[26] Jia C S, Chen T and Cui L G 2009 *Phys. Lett. A* **373** 1621
[27] Zali Z, Amani A, Sadeghi J and Pourhassan B 2021 *Physica B* **614** 413045
[28] Wei G F and Dong S H 2010 *Physica Scripta* **81** 035009
[29] Wei G F and Dong S H 2010 *Euro. Phys. J. A* **46** 207
[30] Qiang W C, Sun G H and Dong S H 2012 *Annalen der Physik* **524** 360
[31] Pedersen T G, Jauho A P and Pedersen K 2009 *Phys. Rev. B* **79** 113406
[32] Zhu W, Wang Z, Shi Q, Szeto K Y, Chen J and Hou J G 2009 *Phys. Rev. B* **79** 155430
[33] Klimchitskaya G L, Mostepanenko V M and Petrov V M 2017 *Phys. Rev. B* **96** 235432
[34] Novoselov K S, Geim A K, Morozov S V, Jiang D E, Zhang Y, Dubonos S V, Grigorieva I V and Firsov A A 2004 *Science* **306** 666
[35] Neto A C, Guinea F, Peres N M, Novoselov K S and Geim A K 2009 *Rev. Mod. Phys.* **81** 109
[36] Nair R R, Blake P, Grigorenko A N, Novoselov K S, Booth T J, Stauber T, Peres N M and Geim A K 2008 *Science* **320** 1308
[37] Chenaghlou A, Aghaei S and Ghadirian Niari N 2021 *Euro. Phys. J. D* **75** 139
[38] Onyenegecha C P, Opara A I, Njoku I J, Udensi S C, Ukewuihe U M, Okereke C J and Omame A 2021 *Results in Physics* **25** 104144
[39] Eshghi M and Mehraban H 2016 *Journal of Mathematical Physics* **57** 082105
[40] Alimohammadian M and Sohrabi B 2020 *Scientific Reports* **10** 1
[41] Downing C A and Portnoi M E 2016 *Phys. Rev. B* **94** 165407
[42] Gupta K S and Sen S 2008 *Phys. Rev. B* **78** 205429
[43] Hassanabadi H, Maghsoodi E, Oudi R, Zarrinkamar S and Rahimov H 2012 *Euro. Phys. J. Plus* **127** 120
[44] Arda A and Sever R 2015 *Commun. Theor. Phys.* **64** 269
[45] Min H, Borghi G, Polini M and MacDonald A H 2008 *Phys. Rev. B* **77** 041407
[46] San-Jose P, Prada E, McCann E and Schomerus H 2009 *Phys. Rev. Lett.* **102** 247204
[47] Tuan D V, Ortmann F, Soriano D, Valenzuela S O and Roche S 2014 *Nat. Phys.* **10** 857